Analytical solutions of velocity profile in flow through submerged vegetation with variable frontal width

Wei-Jie Wang[a], Wen-Xin Huai[b,*], Shuolin Li[c], Ping Wang[d], Yu-Fei Wang[e], Jiao Zhang[b]

[a]*State Key Laboratory of Simulation and Regulation of Water Cycle in River Basin, China Institute of Water Resources and Hydropower Research, Beijing 100038, China.*
[b]*State Key Laboratory of Water Resources and Hydropower Engineering Science, Wuhan University, Wuhan, Hubei 430072, China.*
[c]*Sibley School of Mechanical and Areospace Engineering, Cornell University, Ithaca, NY 14853, USA*
[d]*Key Laboratory of State Forestry Administration on Soil and Water Conservation, School of Soil and Water Conservation, Beijing Forestry University, Beijing 100083, China*
[e]*Department of Civil and Environmental Engineering, Universitat Politècnica de Catalunya (UPC), Barcelona, 08034, Spain*

Abstract

Flow within vegetation is one of the main driving forces for material exchange and energy transfer in wetland systems. Impacted by vegetation, the flow velocity profile illustrates distortions to the classic logarithmic velocity profile and has attracted much attention among researchers. Different from analytical models of velocity distribution in literature, which is mainly suitable for vegetation with uniform frontal width, this paper establishes new analytical solutions of the velocity profile for vegetation such as shrub and sedge that have a variable frontal width in the vertical direction. A new shape function is proposed under these conditions in which the frontal width exhibits a gradual increase in the vertical direction from bottom up in the vegetation. Along with different closure models for eddy viscosity in the vegetation layer and surface layer, analytical solutions of the velocity profile are derived from the momentum equations. Good agreement between calculated and measured data shows

*Corresponding author
Email address: wxhuai@whu.edu.cn (Wen-Xin Huai)

our analytical model is effective in predicting velocity profiles.

Keywords: Analytical solution; Velocity profile; Vegetation; Turbulent flow; Flow resistance.

1. Introduction

Human activities along with the rapid development of society and industrialization have unleashed huge pressure on aquatic ecosystems that include not only the artificial modification of rivers such as projects adopting dams to intercept rivers, cutting and straightening winding rivers, hardening of side slopes and channel bottoms with concrete, but also waste water pollution from agricultural and industrial production. Focusing on these problems, ecological restoration aims to repair damaged water systems and to rebuild healthy aquatic ecosystems to provide a sustainable and healthy development of ecosystems (Li et al., 2015; Yu and Wang, 2014; Mi et al., 2015).

Vegetation is widely used in river and wetland water ecological treatment and restoration (Constança Aguiar, F. et al., 2011; Stromberg, 2001) because it serves many eco-functions, such as fixation through roots for maintaining riverbed stability, water purification through the absorption capacity of the epidermis, and enriching biodiversity features by providing attachment matrices and habitats for organisms.

All of these ecological restoration measures require a description of flow through vegetation, where the flow region is partitioned into different layers according to the dominant vortical structures, resulting in a complex flow pattern (Nepf, 1999; Nepf and Ghisalberti, 2008; Poggi et al., 2004a). How to calculate the flow velocity is a key problem and a fundamental research topic for furthering the studies of contaminant transport and energy loss features. Flow distributions are calculated with two main approaches: numerical models and analytical models. Numerical models, such as direct numerical simulation (DNS), large-eddy simulation (LES), and many others, mainly focus on the local velocity and turbulent features. They yield relatively accurate results

by massive calculations with suitable parameters (Lu and Dai, 2016; Shimizu et al., 1991; Stoesser et al., 2009; Zhang et al., 2013). Sometimes we do not need to focus on each point in the flow region but instead care more about the planar-averaged velocity or bulk velocity for a preliminary prediction. In such instances, an analytical solution with less calculation arises that reveals the principle or bulk law for flow through vegetation. For simplicity, vegetation can always be represented as cylinders or strips (Klopstra et al., 1996; Shimizu et al., 1991; Kouwen et al., 1969; Nepf and Ghisalberti, 2008; Huai et al., 2009; Wang et al., 2018b), and the flow region can be divided into different layers depending on the turbulence model adopted: (1) The one-layer model takes the flow region as a whole, and the friction factor scales with the ratio of vegetation height to flow depth (Cheng, 2015) or scales with the ratio of vegetation-related roughness height to vegetation-related hydraulic radius (Wang et al., 2018c). Interestingly, both scale parameters are around 3/2. (2) In the two-layer model, the flow region is divided into a vegetation layer and a surface layer (Yang and Choi, 2010; Huai et al., 2013), and different momentum equations are proposed for each layer. For rigid dense vegetation, the flow velocity is assumed to be uniform in the vegetation layer and is derived from the momentum balance between the vegetation drag and the gravity component(Yang and Choi, 2010; Baptist et al., 2007). Furthermore, the velocity at the surface layer is expressed by a logarithmic formula with zero-plane displacement(Thom, 1971). For flexible vegetation, the bending of the stem was considered by Huai et al. (2013) with two kinds of resistance force, specifically, drag force and friction force. These forces scale with the square of the flow velocity, and an analytical solution was proposed by solving the momentum equation in each layer. Further investigation showed that a linear drag–velocity relation occurs when bending is very large (Wang et al., 2015b). (3) In the multiple-layer model, a sub-layer occupying a very thin layer near the bottom of the channel is separated from the vegetation layer (Baptist et al., 2007), and an additional layer called the mixing layer, which is separated from both the vegetation layer and the surface layer near the top of the vegetation (Okamoto and Nezu, 2009; Katul et al., 2002;

Nepf, 2012; Ghisalberti and Nepf, 2002), where the flow features are related to the frequency of the Kelvin–Helmholtz instability (Peters, 2012). Moreover, vegetation in this research has the same height, whereas vegetation in nature is always non-uniform in height. Research was conducted on this topic (Huai et al., 2014; Liu et al., 2010), in which a combination of the aforementioned two-, three- or multiple-layer model was adopted and improved for different vegetation heights.

In some manner, a solution of the velocity profile is adopted for determining the resistance of the vegetated channel when solving the Saint-Venant equations (SVEs) describing water flow. As is well-known, there is a need for the closure of the energy slope S_f, for the flow, which may be derived from the force balance with a 'local uniform' assumption (Thompson et al., 2011; Wang et al., 2015a, 2018a). When dealing with open channel flow without obstacles, the classic Manning formula is adopted,

$$S_f = (\frac{2gn^2}{R^{4/3}})\frac{U_b^2}{2g}, \tag{1}$$

where g is acceleration due to gravity, n Manning's coefficient of roughness, U_b the bulk velocity for whole flow depth, and R the hydraulic radius. For flow within the vegetation, the energy slope S_f is complicated and may be derived from a force balance equation. Our previous work (Wang et al., 2015a) derived an equation for the flow through emergent vegetation for a given length-scale dx along the streamwise direction,

$$\gamma B h_w dx(1-\phi)S_f = BdxF_{d,bulk} + Bdx(1-\phi)\tau_{ground} + 2h_w dx\tau_{wall}, \tag{2}$$

where γ denotes the bulk density of water, B channel width, h_w flow depth, ϕ the area concentration of vegetation stems, $F_{d,bulk}$ the vegetation form drag per unit ground area, τ_{ground} friction along the bottom of the channel, and τ_{wall} friction along the sidewall of the channel. For flow through vegetation, friction along the sidewall and bottom can always be ignored Wang et al. (2015a), resulting in a balance between the streamwise gravity and form drag of vegetation as

$$\gamma h_w(1-\phi)S_f = F_{d,bulk}, \tag{3}$$

where the form drag acting on the unit ground area is calculated from

$$F_{d,bulk} = C_d A_{frontal} \frac{\rho U_b^2}{2}, \tag{4}$$

with C_d the drag coefficient and $A_{frontal}$ the total frontal area of vegetation stems per unit bed ground, obtained using

$$A_{frontal} = mDh_w, \tag{5}$$

where m is the vegetation density, denoting the number of vegetation stems per unit bed ground, and D the frontal width for a single stem. The bulk form drag in equation 3 then becomes

$$F_{d,bulk} = C_d mDh_w \frac{\rho U_b^2}{2}. \tag{6}$$

For submerged vegetation, the flow region is divided into two layers (vegetation layer and surface layer). The drag in the vegetation layer is expressed by

$$F_{d,bulk} = C_d mDh_v \frac{\rho U_v^2}{2}, \tag{7}$$

where h_v is the vegetation height and U_v the depth-averaged velocity for the vegetation layer.

The closure of S_f for emergent vegetation in flow is then

$$S_f = (\frac{C_d mD}{1-\phi}) \frac{U_b^2}{2g}, \tag{8}$$

and for submerged vegetation is

$$S_f = [\frac{C_d mDh_v}{(1-\phi)h_w}] \frac{U_v^2}{2g}. \tag{9}$$

All considered, the velocity profile is key for the description of fluid motion. However, several analytical models exist that have been derived for simplified vegetation models, i.e., a cylinder or single strip with a constant frontal width limited by the solvability of the momentum equation. Different from existing studies on analytical models of velocity distribution with a uniform frontal width of vegetation, the main innovative points of this paper are: (1) a new shape

function describing frontal width of the vegetation array; (2) new solutions of the velocity profile derived from momentum equations taking into account vegetation shape; and (3) new empirical expressions for parameters in solutions are provided. Comparison between modeled results and measured ones proves that the new solutions proposed here are effective for predicting velocity profiles in vegetated flows.

2. Theory

2.1. Governing equations

For steady, fully developed turbulent flow with vegetation, the flow region is divided into two layers: the vegetation layer and the surface layer (Fig. 1). In the Navier–Stokes momentum equation, the vegetation drag is considered as a body force in the vegetation layer. Choosing Cartesian coordinates, we define the streamwise direction as x, the transverse direction as y, and the vertical direction as z, with velocity components $\boldsymbol{V} = (u, v, w)$ corresponding to the coordinate directions (x, y, z). Then, for a control volume, its governing equation is expressed in the streamwise direction as follows:

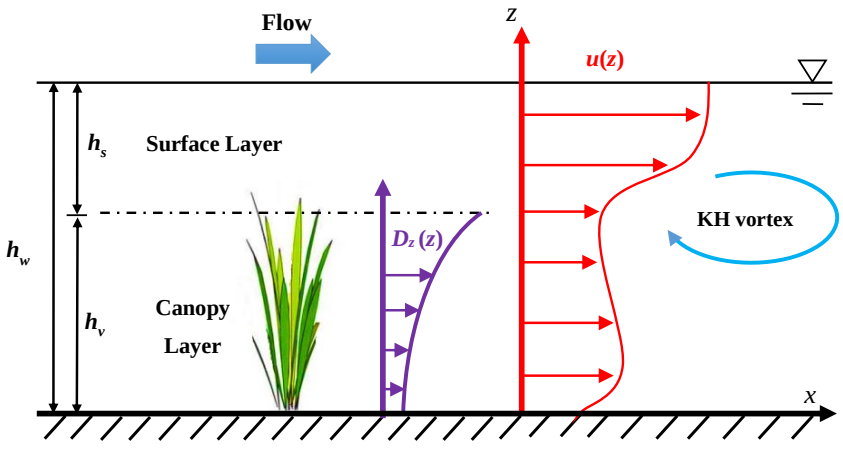

Figure 1: Sketch of flow through vegetation with non-uniform frontal width in the vertical direction

$$\frac{Du}{Dt} = f_x - \frac{1}{\rho}\frac{\partial p}{\partial x} + \nu\left(\frac{\partial^2 u}{\partial x^2} + \frac{\partial^2 u}{\partial y^2} + \frac{\partial^2 u}{\partial z^2}\right), \tag{10}$$

where f_x is the force acting on the control volume indicating the body force per unit mass, p pressure, and ν kinematic viscosity.

The Reynolds-averaged approach applied to the above governing equation gives

$$\frac{D\overline{u}}{Dt} = \overline{f_x} - \frac{1}{\rho}\frac{\partial \overline{p}}{\partial x} + \nu\left(\frac{\partial^2 \overline{u}}{\partial x^2} + \frac{\partial^2 \overline{u}}{\partial y^2} + \frac{\partial^2 \overline{u}}{\partial z^2}\right) + \left(\frac{\partial(-\overline{u'u'})}{\partial x} + \frac{\partial(-\overline{u'v'})}{\partial y} + \frac{\partial(-\overline{u'w'})}{\partial z}\right), \tag{11}$$

which can be reduced to the following form when focusing on the streamwise direction

$$\frac{D\overline{u}}{Dt} = \overline{f_x} - \frac{1}{\rho}\frac{\partial \overline{p}}{\partial x} + \frac{1}{\rho}\frac{\partial \tau}{\partial z}, \tag{12}$$

where the total shear stress τ, including viscous stress (which can always be ignored for turbulent flow) and Reynolds stress, is expressed as

$$\tau = \rho\nu\frac{\partial \overline{u}}{\partial z} - \rho\overline{u'w'}, \tag{13}$$

with $-\rho\overline{u'w'}$ the Reynolds stress. The planar-averaged momentum equation for vegetated flow is then described as (Klopstra et al., 1996; Baptist et al., 2007; Liu et al., 2012; Huai et al., 2009; Poggi et al., 2009; Katul et al., 2011; Wang et al., 2015b)

$$G_x + \delta F_d + \frac{1}{\rho}\frac{\partial \tau}{\partial z} = 0, \tag{14}$$

where $G_x = gS_o$ is the gravitational component in the streamwise direction, S_o the bed slope, parameter $\delta = -1$ denoting the vegetation layer and $\delta = 0$ the surface layer, F_d denotes the drag from the canopy acting on the control volume (different from the above mentioned $F_{d,bulk}$) and is calculated using

$$F_d = \frac{1}{2}C_d m D_z [u(z)]^2, \tag{15}$$

where D_z is the frontal width of the vegetation stem (here the subscript z signifies that this frontal width may vary with vertical direction z).

2.2. Models for shear stress

To solve the momentum equation, the model for shear stress is the key component and has been investigated by many researchers. One should note that viscous stress can always be ignored for turbulent flow (Baptist et al., 2007; Luhar et al., 2008; Liu et al., 2012; Huai et al., 2014). Several models or theories have been proposed. They fall into two categories: non-differential and differential formulas.

2.2.1. Non-differential formulas for shear stress

For the non-differential formula, Shimizu et al. (1991) indicates that Reynolds stress follows an exponential profile for the vegetation layer, and this feature was confirmed in Dijkstra and Uittenbogaard (2010), in which the data displayed a similar trend with a peak value at the vegetation top. This trend was also validated in experiments for rigid (Huai et al., 2009) and flexible vegetation (Huai et al., 2013), and can be expressed in the form

$$\tau_v = \tau_{max}\exp[\alpha(z - h_v)], \tag{16}$$

where subscript 'v' of the shear stress τ signifies the vegetation layer, α denotes a constant to be determined by the boundary conditions, and $\tau_{max} = gS_o h_s$ is the peak value for shear stress at the top of the vegetation, $h_s = h_w - h_v$ being the height of the surface layer.

2.2.2. Differential formula for shear stress

For the differential formula of shear stress, the classic Boussinesqs eddy viscosity approach yields

$$\tau = \rho\nu_t \frac{\partial u(z)}{\partial z}, \tag{17}$$

where ν_t is the eddy viscosity. Considered constant by Boussinesq in earlier years, a large body of experimental result indicate a variational behavior for eddy viscosities that depend on flow conditions. Theories for describing a variable eddy viscosity are summarized in the following:

(i) Classic von Kármán–Prandtl mixing-length theory shows the eddy viscosity is linked with the velocity gradient as

$$\nu_t = l^2 |\frac{\partial u(z)}{\partial z}|, \tag{18}$$

where the mixing lengths $l = \kappa z$, $\kappa = 0.41$ is the Kármán constant, which is widely used in channel flow in the absence of vegetation. Further investigations (Katul et al., 2011; Poggi et al., 2004b,a) showed that the mixing length is associated with the size of the vortex for different zones when vegetation is present. In the vegetation layer, the mixing length may be calculated using $l = 2\beta^3 L_c$, where $\beta = u_*/u(h_v)$ is the coefficient of momentum absorption, and the friction velocity is $u_* = \sqrt{gS_o h_s}$. For the surface layer, the mixing length is described by $l = \kappa(z - d)$, where d is the zero-plane displacement, which is defined by Thom (1971) adopting $d = \int_0^{h_v} \frac{d\tau}{dz} z dz / \int_0^{h_v} \frac{d\tau}{dz} dz$ and can be calculated using the formula from Katul et al. (2011) with $d = h_v - 2\beta^3 L_c/\kappa$, where $L_c = (C_d a)^{-1}$ is the adjustment length scale (Belcher et al., 2003), indicating the loss of turbulent kinetic energy from advecting eddies due to vegetation (Katul et al., 2004), $a \approx LAI/h_v$ is the mean leaf area density, and LAI the one-sided leaf area index.

(ii) Aside from the differential formula for eddy viscosity, several researchers have proposed that eddy viscosity is linked with the friction velocity times an adjusted length scale (Wang, 2012; Wang et al., 2015b)

$$\nu_t = l u_*. \tag{19}$$

or the velocity multiplied by an adjusted length scale (Baptist et al., 2007)

$$\nu_t = (c_p l) u, \tag{20}$$

where c_p is the intensity of turbulence calculated based on the turbulent kinetic energy k_t and velocity $u(z)$. Further investigations have found that the product of turbulence c_p and mixing length l does not vary with vertical height z (Liu et al., 2012; Van Velzen et al., 2003), expressed as a function of layer height

$$c_p l = 0.015\sqrt{h_v h_w}, \tag{21}$$

and this expression was improved by Baptist et al. (2007), adopting the data of Nepf and Vivoni (2000) to obtain

$$c_p l = \frac{h_s}{20}. \tag{22}$$

In the following derivation, the eddy viscosity of type (ii) (equations 19 and 20) was adopted in the momentum equations in solving the velocity distribution. The empirical equations for $c_p l$ from different research groups (equations 21 and 22) were later tested.

2.3. Velocity solution in the vegetation layer

Considering the solvability of the momentum equation, and with the adoption of equation (20), shear stress is expressed as

$$\tau_v = c_p l \rho u(z) \frac{\partial u(z)}{\partial z}. \tag{23}$$

Then the momentum equation gives

$$\frac{1}{2} c_p l \frac{\partial^2 [u(z)]^2}{\partial z^2} - \frac{1}{2} C_d m D_z [u(z)]^2 + g S_o = 0, \tag{24}$$

which takes the form

$$p_1 \frac{\partial^2 [u(z)]^2}{\partial z^2} + p_2 D_z [u(z)]^2 + p_3 = 0, \tag{25}$$

with the introduction of parameters

$$p_1 = \frac{1}{2} c_p l, \tag{26}$$

$$p_2 = -\frac{1}{2} C_d m, \tag{27}$$

$$p_3 = g S_o. \tag{28}$$

(i) For vegetation with uniform vertical width, $D_z = D_0$ is a constant, and the analytical solution of velocity profile gives

$$u_v(z) = \sqrt{c_1 \exp\left(\sqrt{-\frac{p_2}{p_1}} D_0 z\right) + c_2 \exp\left(-\sqrt{-\frac{p_2}{p_1}} D_0 z\right) - \frac{p_3}{p_2 D_0}}. \tag{29}$$

(ii) For vegetation with width-varying shape, here we take shrub and sedge as representative (Liu et al., 2011, 2012; Huai et al., 2019), where the frontal width increases from bottom up (narrow at the bottom and wide near the top of the vegetation). Liu et al. (2011, 2012) proposed two shape functions to describe the effect of variable frontal width in flow the first being

$$D_z = \frac{(1-2n_1)D_{max}}{4(n_1 z/n_2 + n_3)^2}, \tag{30}$$

and the second

$$D_z = [\frac{n_4 z + n_5}{n_6 z^2 + n_7 z + n_8}]^2 D_{max}, \tag{31}$$

where n_i $(i = 1, 2, 3..., 8)$ are parameters to be determined from vegetation morphotype and flow characteristics, and D_{max} is the maximum frontal width of vegetation. Three or five parameters are needed to build the shape of the vegetation array in these two approaches. From another point of view, these parameters include not only the physical attributes of the vegetation (frontal width), but also flow features such as turbulence intensity C_p, drag coefficient C_d, and mixing length scale l. Here, considering the solvability of the governing equation, a new shape function is proposed that only focuses on the physical shape of the vegetation. Requires just two parameters, we have

$$D_z = (q_1 z + q_2)^{-2}, \tag{32}$$

where q_1 and q_2 are determined by the physical shape of the vegetation. Assuming the vegetation gradually widens from bottom up, which is very common in nature (Liu et al., 2012), expressions for q_1 and q_2 linked with vegetation attributes were obtained,

$$q_1 = \frac{D_{max}^{-1/2} - D_{min}^{-1/2}}{h_v}, \tag{33}$$

and

$$q_2 = D_{min}^{-1/2}, \tag{34}$$

where D_{min} is the minimum width at the bottom.

Then the momentum equation (equation 25) with variable width (equation 32) was solved analytically to get the velocity distribution in the vegetation layer

$$u_v(z) = \sqrt{c_3(q_1 z + q_2)^{L_1} + c_4(q_1 z + q_2)^{L_2} + c_5(q_1 z + q_2)^2}, \tag{35}$$

where

$$L_1 = \frac{q_1\sqrt{p_1} + \sqrt{p_1 q_1^2 - 4p_2}}{2q_1\sqrt{p_1}}, \tag{36}$$

$$L_2 = \frac{q_1\sqrt{p_1} - \sqrt{p_1 q_1^2 - 4p_2}}{2q_1\sqrt{p_1}}, \tag{37}$$

$$c_5 = \frac{4p_3}{p_1 q_1^2 - 4p_2 - 9q_1^2 p_1}, \tag{38}$$

where c_3 and c_4 are integration constants determined by the boundary conditions.

The parameters in the shape function also can be determined by boundary conditions. When $z = 0$, the slip velocity is

$$u_{slip} = \sqrt{c_3(q_2)^{L_1} + c_4(q_2)^{L_2} + c_5(q_2)^2}, \tag{39}$$

which is calculated from the momentum balance at the bottom of the channel

$$u_{slip} = \sqrt{\frac{2gS_f}{C_d m D_{min}}}, \tag{40}$$

where S_f is the energy slope.

From the momentum balance, the interfacial shear stress between the vegetation layer and the surface layer establishes another boundary condition at the top of the canopy (Klopstra et al., 1996; Wang et al., 2015b; Yang and Choi, 2010). When considering the shear stress in the vegetation layer at $z = h_v$,

$$\tau_v|_{z=h_v} = \rho c_p l \cdot \left[u(z)\frac{\partial u(z)}{\partial z}\right]\Big|_{z=h_v}. \tag{41}$$

The shear stress in the surface layer at $z = h_v$ is

$$\tau_s|_{z=h_v} = \rho g h_s S_f. \tag{42}$$

Then, parameters c_3 and c_4 are obtained by solving the momentum equation combined with these two boundary conditions,

$$c_3 = -\frac{q_2^{L_2}\left[c_5\left(c_p l\right) q_1\left(h_v q_1 + q_2\right) - g h_s S_f\right] - \frac{1}{2}\left(c_p l\right) L_2 q_1 \left(c_5 q_2^2 - u_{slip}^2\right)\left(h_v q_1 + q_2\right)^{L_2 - 1}}{\frac{1}{2}\left(c_p l\right) L_1 q_1 q_2^{L_2}\left(h_v q_1 + q_2\right)^{L_1 - 1} - \frac{1}{2}\left(c_p l\right) L_2 q_1 q_2^{L_1}\left(h_v q_1 + q_2\right)^{L_2 - 1}}, \tag{43}$$

$$c_4 = \frac{q_2^{L_1 - L_2}\left\{q_2^{L_2}\left[c_5\left(c_p l\right) q_1\left(h_v q_1 + q_2\right) - g h_s S_f\right] - \frac{1}{2}\left(c_p l\right) L_2 q_1 \left(c_5 q_2^2 - u_{slip}^2\right)\left(h_v q_1 + q_2\right)^{L_2 - 1}\right\}}{\frac{1}{2}\left(c_p l\right) L_1 q_1 q_2^{L_2}\left(h_v q_1 + q_2\right)^{L_1 - 1} - \frac{1}{2}\left(c_p l\right) L_2 q_1 q_2^{L_1}\left(h_v q_1 + q_2\right)^{L_2 - 1}}$$

$$\text{-}q_2^{-L_2}\left(c_5 q_2^2 - u_{slip}^2\right). \tag{44}$$

2.4. Velocity solution in the surface layer

For flow in the surface layer ($z > h_v$), the traditional method adopts the logarithmic function with

$$u_s(z) = \frac{u_*}{\kappa}\ln(\frac{z-d}{z_0}), \tag{45}$$

where two parameters are needed such as roughness height z_0 and zero-plane displacement d.

Here, we adopt another approach to predict velocity that needs only one parameter to shape the velocity profile. First, the momentum equation for surface layer gives

$$\frac{\partial \tau_s}{\partial z} + \rho g S_o = 0, \tag{46}$$

where the shear stress adopted equation (19) with mixing length $l = k_n z$, and k_n is a coefficient determined by the flow characteristics and vegetation attributes

$$\tau_s = \rho k_n u_* z \frac{\partial u(z)}{\partial z}, \tag{47}$$

where subscript 's' to the shear stress denotes the surface layer. Then, the analytical solution is obtained by substituting equation (47) into (46) yielding

$$u_s(z) = -\frac{g S_o}{k_n u_*} z + c_6 \ln z + c_7, \tag{48}$$

where parameters c_6 and c_7 are constants determined by the following two boundary conditions.

Boundary condition (i): the velocity at the top of the canopy in the surface layer and the vegetation layer is the same

$$u_v(h_v) = u_s(h_v). \tag{49}$$

Boundary condition (ii): the velocity gradient is zero at the flow surface

$$\left.\frac{\partial u(z)}{\partial z}\right|_{z=h_w} = 0. \tag{50}$$

One obtains then parameters values

$$c_6 = \frac{g h_w S_o}{k_n u_*}, \tag{51}$$

$$c_7 = \frac{g S_o (h_v - h_w \ln h_v) + k_n u_* \sqrt{c_3 (h_v q_1 + q_2)^{L_1} + c_4 (h_v q_1 + q_2)^{L_2} + c_5 (h_v q_1 + q_2)^2}}{k_n u_*}. \tag{52}$$

Next, the flow profile in the surface layer is described by equation (48). The approach in determining parameter k_n is discussed in Section 4.

3. Experiments

We conducted flume experiments in an open channel using modelled plants for simulating variable-width vegetation. Moreover, two set of experimental data from the literature were included to enrich the scope of the experimental data. Their details are described in the following.

3.1. Present experiments

Experiments were conducted in two glass channels at the State Key Laboratory of Water Resources and Hydropower Engineering Science in Wuhan University, China (details are given in Huai et al. (2019)). The size of these two channels were: 20 m long × 0.6 m wide × 0.4 m deep (bed slope 0.04%) and 20 m long × 1.0 m wide × 0.4 m deep (bed slope 0.01%). The channels were equipped with electro-magnetic flow meters for measuring flow discharge, and a tailgate located at the end of the channels to control flow depth. The vegetation was installed in a staggered arrangement along the bottom of the channel. The

length of vegetation zone was set to 8 m to ensure a complete development of the flow within and above the vegetation.

For the simulated vegetation in this experiment, a meadow model plant was adopted to represent sedge. Each plant has 11 plastic slips and the diameter of the trunk was approximately 0.015 m. The original averaged height of the sedge meadow model was 0.210 m, and the lateral width ranged from $D_{min} = 0.02$ m (at the bottom) to $D_{max} = 0.170$ m (near the top). The artificial vegetation produced a small deflection because of its flexibility.

Velocity measurements were taken using an acoustic Doppler velocimeter. For model verification in Section 4, the velocity profile at the location where $x/L_{veg} > 0.61$ was selected, at which point the flow reaches its fully developed condition (Huai et al., 2019).

3.2. Liu et al.'s experiments

Liu et al. (2011, 2012) conducted a series of experiments at the Hydraulic laboratory of Tsinghua University, China. They modeled shrub-like vegetation in an open channel 22.6 m long × 1.6 m wide × 0.8 m deep, with a bed slope of 0.67 %. The average height of the shrubs was 0.275 m, with an increasing trend for the frontal width along the vertical direction from the bottom up. Here, $D_{min} = 0.05$ m near the bottom (this value was not given in their publication but can be reasonably estimated from their photographs), and $D_{max} = 0.200$ m near the top of the vegetation. The vegetation was fixed in a staggered arrangement with two distinct canopy densities: $m = 15.71$ and 7.85 stems/m^2. The velocity profile was measured using an acoustic Doppler velocimeter.

3.3. Nepf and Vivoni's experiments

Nepf and Vivoni (2000) conducted experiments with a 24 m long × 0.38m wide recirculating glass wall flume. The model vegetation zone was 7.4 m long with a height of 0.16 m, with a staggered arrangement of plants (vegetation density was $m = 330$ stems/m^2). In addition, according to the principle proposed by Kouwen and Li (1980), their vegetation was constructed based on similarity

Table 1: Summary of present research on flow in vegetation

Data type	Present experiments			Liu et al.		Nepf and Vivoni
	Case 1	Case 2	Case 3	Case 1	Case 2	Case 1
Flow depth, h_w (m)	0.27	0.27	0.33	0.45	0.45	0.44
Adjusted vegetation height, h_v(m)	0.165	0.175	0.190	0.255	0.255	0.14
Max width, D_{max}(m)	0.17	0.17	0.17	0.2	0.2	0.017
Min width, D_{min} (m)	0.02	0.02	0.02	0.05	0.05	0.005
Vegetation density, m (stems/m^2)	43.3	108.3	108.3	15.71	7.85	330
Drag coefficient C_d	0.13	0.17	1.3	1.5	1.5	0.5
Turbulence scale, $c_p l$ ($\times 10^{-4}$ m)	5	4.5	12	30	32	10
Turbulence index, k_n ($\times 10^{-3}$)	40	40	50	50	45	60

in geometry and flexural rigidity to prototype aquatic vegetation. Each plant consisted of six blades, each of width 0.003 m. The morphology of a single plant featured a variable frontal width ranging from 0.005 to 0.017 m.

3.4. Summary of experimental parameters

The experimental setup and vegetation attributes are listed in Table 1. As there were waves near the top of the vegetation resulting in a greatly reduced resistance at this point, an adjusted vegetation height was proposed where the height was slightly lower (0.02 m) than the reported vegetation height. Moreover, note that some parameters, such as flow depth of the experiments of Liu et al. (2012)'s were not given and hence we estimated values from velocity profiles of their paper (Although there may be minor errors, such errors would have little effect on the final calculation).

4. Results and discussion

This section is divided into three subsections: (1) A comparison of the analytical velocity solutions for the whole depth with measured data is discussed in Section 4.1; (2) Features of the drag coefficient are discussed in Section 4.2; and (3) turbulence features are discussed in Section 4.3.

4.1. Velocity profile comparisons

A comparison between the analytical solutions of the velocity profile (adopting best-fitted parameters, which will be discussed later) and measured data is shown in Fig. 2. The solution proposed here is seen to reproduce well the velocity profile for flow through vegetation with variable frontal width. The following subsections present the procedure used in deriving the empirical expressions for the adjusted parameters.

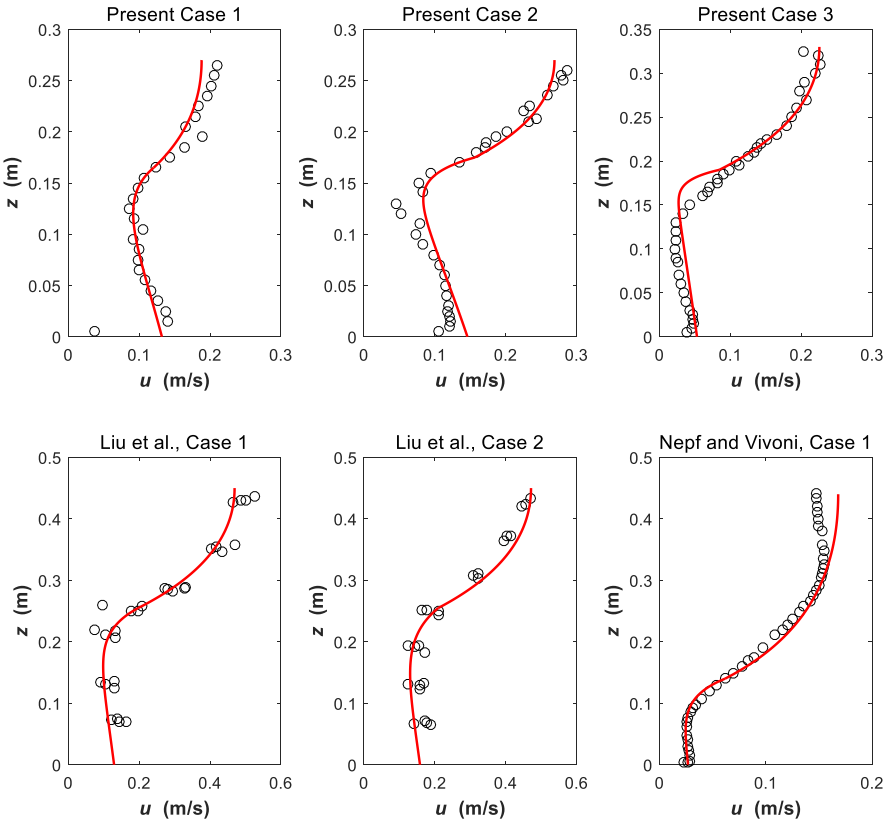

Figure 2: Comparison of analytical solutions with measured data for different cases

4.2. Features of the drag coefficient

Drag coefficient C_d is a key factor for quantifying the resistance to flow (Nepf and Ghisalberti, 2008; Wang et al., 2018a; Baptist et al., 2007). For an isolated cylinder, the local C_d can be calculated from (Cheng, 2012)

$$C_{d,iso} = 11Re_d^{-0.75} + 0.9\Gamma_1\left(Re_d\right) + 1.2\Gamma_2\left(Re_d\right), \tag{53}$$

where

$$\Gamma_1\left(Re_d\right) = 1 - \exp\left(-\frac{1000}{Re_d}\right), \tag{54}$$

and

$$\Gamma_2\left(Re_d\right) = 1 - \exp\left[-\left(\frac{Re_d}{4500}\right)^{0.7}\right], \tag{55}$$

where the Reynolds number for a cylinder is $Re_d = Ud/\nu$ with U the approaching velocity. However, for flow through a vegetation array ('array' means more than just a single stem in the flow), resistance mechanisms become complicated, and the C_d of a vegetated array differs much from an isolated stem ($C_{d,iso}$). When only considering the effect of vegetation density on the drag coefficient, C_d displays an increasing trend (Tanino and Nepf, 2008; Stoesser et al., 2010) or a decreasing trend (Nepf, 1999; Lee et al., 2004) when increasing the vegetation density (Etminan et al., 2017). This indicates that the drag due to the vegetation array cannot be assessed by only the vegetation density. Hence a vegetation-related Reynolds number is introduced, $Re_v = (R_v/D)Re_d$. Many experiments show a monotonic decline in C_d with increasing vegetation-related Reynolds number (Re_v) for canopies composed of cylinders (Ishikawa et al., 2000; James et al., 2004; Tanino and Nepf, 2008; Liu et al., 2008; Ferreira et al., 2009; Kothyari et al., 2009; Stoesser et al., 2010), which can be expressed as (Wang et al., 2019)

$$C_{d,wang} = 0.819 + \frac{58.5}{\sqrt{\frac{\pi(1-\phi)}{4\phi}Re_d}}. \tag{56}$$

Due to the variation of D_z in the vertical direction, there is a need to calculate the averaged width D_{ave} when adopting these formulas (equations 53 and

385 56). Based on shape function (equation 32), the averaged width is calculated
386 from

$$D_{ave} = \frac{1}{q_2(q_1 h_v + q_2)}. \tag{57}$$

387 Then, the Reynolds number for vegetation with variable frontal width reads

$$Re_d = \frac{U_v D_{ave}}{\nu}, \tag{58}$$

388 where U_v is the averaged velocity for the vegetation layer.

389 Although the above formula of C_d was mainly derived based on cylinder
390 or strip with constant width D, the left and middle panels in Fig. 3 illustrate
391 that the predicted C_d using equations (53) and (56) deviates from the measured
392 value, and shows that they are not suitable for vegetation with variable D_z,
393 where the measured C_d is obtained by matching the calculated velocity profile
394 to the measured value. Hence the drag coefficient C_d here needs to reflect the
395 above-mentioned vegetation shape with D_{min} and D_{max}. The following formula
396 was proposed by incorporating the traditional Reynolds number in with the
397 plant morphology descriptors

$$C_{d,new} = \frac{Re_d}{1110}\left(\frac{2D_{\min} - D_{ave}}{D_{ave}}\right) + \left(\frac{51.4D_{ave} - 9.85D_{\max} - 60.5D_{\min}}{D_{ave}}\right). \tag{59}$$

398 A comparison between measured and the newly derived empirical drag coeffi-
399 cient (right panel of figure 3) show good agreement proving that equation 59
400 matches the measured value very well.

401 *4.3. Turbulence features*

402 *4.3.1. Vegetation layer*

403 The turbulence scale $c_p l$ derived in previous studies on vegetation flow with
404 cylinders or stripes shows a dependence on layer height (equations 21 and 22).
405 However, comparisons between the measured $C_p l$ with values from these two
406 equations show that they are not suitable for vegetation of distinct shape (see
407 left and middle panels of Fig. 4). Based on the height of each layer, a new

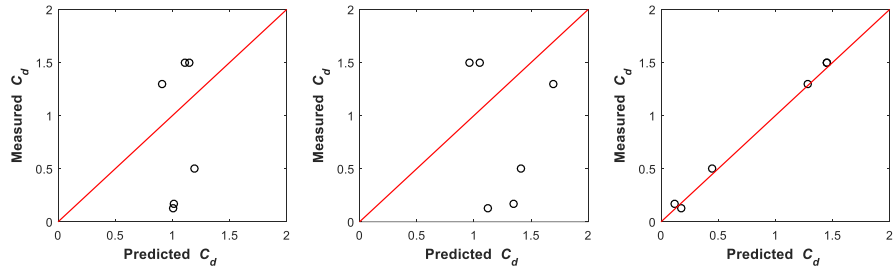

Figure 3: Comparison between measured and predicted drag coefficients. The predicted C_ds given in the left, middle, and right panels are $C_{d,iso}$ from equation (53), $C_{d,wang}$ from equation (56), and $C_{d,new}$ from equation (59), respectively.

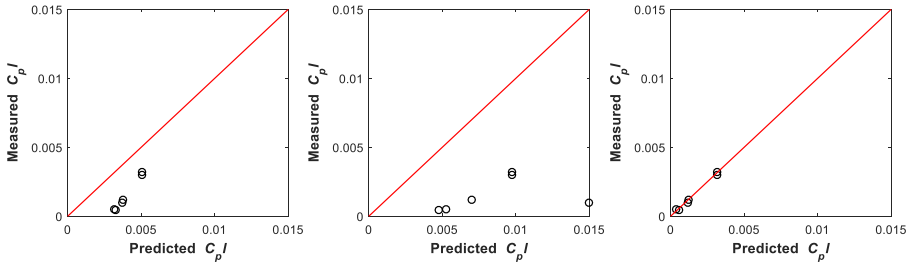

Figure 4: Comparison between measured and predicted formula for turbulence length scale $c_p l$ in the vegetation layer. The predicted $C_p l$ for the left, middle, and right panels are obtained from equations (21) and (22), and proposed equation (60), respectively.

empirical expression is proposed for the vegetation with variable frontal width, specifically

$$c_p l = \frac{1}{42} h_w - \frac{1}{60} h_s - \frac{1}{233}. \tag{60}$$

A comparison (right panel of Fig. 4) shows that this formula is in good agreement with the measured turbulence length scale for the instance discussed here.

4.3.2. Surface layer

The traditional logarithmic formula (equation 45) describes the flow profile of the surface layer with two parameters: zero-plane displacement d and hydrodynamic roughness height z_0. We now adopt another approach which only

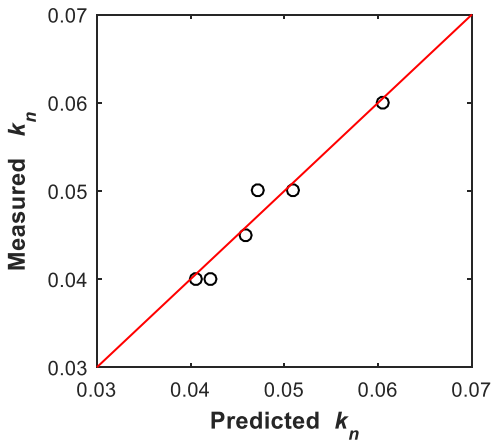

Figure 5: Comparison between measured and predicted turbulence index k_n in surface layer.

needs one parameter k_n for shaping the velocity profile (equation 48). This k_n is seen as a combination of d and z_0 but is complicated and influenced by many factors. Here, for simplicity, dimensionless h_v/L_c (including the vegetation attribute and resistance length scale of vegetation) and the ratio of layer height are taken as influence factors, yielding the following fitted expression

$$k_n = \frac{2}{25} + \frac{1}{310}\frac{h_v}{L_c}\frac{h_v}{h_s} - \frac{1}{16}\frac{h_v}{h_w}. \tag{61}$$

A comparison between measured and predicted k_n is shown in Fig. 5, indicating that the proposed formula well matches the turbulence index k_n for instances reported above.

4.4. Limitations

Although the shape function proposed in equation (32) illustrates a gradual increasing trend in frontal width D_z from bottom up and is suitable for vegetation such as shrub and sedge, the investigation needs to be broadened to other types of vegetation. Moreover, although empirical expressions for the three parameters C_d, $c_p l$, and k_n were proposed for various instances studied here,

further investigation is still needed in considering different vegetation shapes and flow conditions.

5. Conclusion

Different from former analytical models of velocity distribution in literature, which is mainly suitable for vegetation stems with uniform frontal width, this study established new analytical solutions of the velocity profile for vegetation with shape. A brief summary of results is presented in the following:

(1) Vegetation such as shrub and sedge of certain shape where the frontal width D_z displays a gradual increasing trend with vertical direction from the bottom up was investigated. A new vegetation shape function describing the frontal width D_z was proposed linked with D_{max} and D_{min} and needs fewer parameters than previous formulas.

(2) Different closure models for eddy viscosity were adopted for the two-layer vegetated flow, where eddy viscosity was expressed as a product of velocity scaled by an adjusted length scale in the vegetation layer and the friction velocity scaled by an adjusted length scale in surface layer. Combined with the proposed shape function describing frontal width of vegetation, analytical solutions of the velocity profile were derived from the momentum equations. Good agreement between calculated and measured data shows the analytical model is effective for predicting velocity profile.

(3) Because the shape of vegetation is different from the simplified vegetation models using cylinders or single strips, the former empirical formulas of the drag coefficient and the turbulence length scale were not suitable for the width-varying vegetation here. New empirical expression were proposed that matched the observed data well.

(4) There were few experiments focused on width-varying vegetation up to now. Although empirical expressions for determining parameters such as drag coefficient C_d, turbulence length scale for vegetation layer $c_p l$, and surface layer k_n were proposed for a number of limited scenarios, further investigation and

more experiments are needed in considering different vegetation types and flow conditions.

Acknowledgments

The authors acknowledge support through the following projects: National Natural Science Foundation of China (51809286, 51439007, 11672213, and 11872285); Research and Development Support Program of China Institute of Water Resources and Hydropower Research (WE0145B062019); and China Postdoctoral Science Foundation (2017M610949 and 2018T110122).

References

Baptist, M., Babovic, V., Rodríguez Uthurburu, J., Keijzer, M., Uittenbogaard, R., Mynett, A., Verwey, A., 2007. On inducing equations for vegetation resistance. Journal of Hydraulic Research 45, 435–450. doi:10.1080/00221686.2007.9521778.

Belcher, S.E., JERRAM, N., HUNT, J.C.R., 2003. Adjustment of a turbulent boundary layer to a canopy of roughness elements. Journal of Fluid Mechanics 488, 369–398.

Cheng, N.S., 2012. Calculation of drag coefficient for arrays of emergent circular cylinders with pseudofluid model. Journal of Hydraulic Engineering 139, 602–611. doi:10.1061/(ASCE)HY.1943-7900.0000722.

Cheng, N.S., 2015. Single-layer model for average flow velocity with submerged rigid cylinders. Journal of Hydraulic Engineering doi:10.1061/(ASCE)HY.1943-7900.0001037.

Constança Aguiar, F., Rosário Fernandes, M., Teresa Ferreira, M., 2011. Riparian vegetation metrics as tools for guiding ecological restoration in riverscapes. Knowl. Managt. Aquatic Ecosyst. , 21URL: https://doi.org/10.1051/kmae/2011074, doi:10.1051/kmae/2011074.

Dijkstra, J., Uittenbogaard, R., 2010. Modeling the interaction between flow and highly flexible aquatic vegetation. Water Resources Research 46. doi:10.1029/2010WR009246.

Etminan, V., Lowe, R.J., Ghisalberti, M., 2017. A new model for predicting the drag exerted by vegetation canopies. Water Resources Research 53, 3179–3196. URL: http://dx.doi.org/10.1002/2016WR020090, doi:10.1002/2016WR020090.

Ferreira, R.M., Ricardo, A.M., Franca, M.J., 2009. Discussion of "laboratory investigation of mean drag in a random array of rigid, emergent cylinders"

494 by yukie tanino and heidi m. nepf. Journal of Hydraulic Engineering 135,
495 690–693. doi:10.1061/(ASCE)HY.1943-7900.0000021.

496 Ghisalberti, M., Nepf, H.M., 2002. Mixing layers and coherent structures in
497 vegetated aquatic flows. Journal of Geophysical Research 107, 3011. doi:10.
498 1029/2001JC000871.

499 Huai, W.X., Wang, W.J., Hu, Y., Zeng, Y.H., Yang, Z.H., 2014. Analytical
500 model of the mean velocity distribution in an open channel with double-
501 layered rigid vegetation. Advances in Water Resources 69, 106–113. doi:doi.
502 org/10.1016/j.advwatres.2014.04.001.

503 Huai, W.X., Wang, W.J., Zeng, Y.H., 2013. Two-layer model for open channel
504 flow with submerged flexible vegetation. Journal of Hydraulic Research 51,
505 708–718. doi:10.1080/00221686.2013.818585.

506 Huai, W.X., Zeng, Y.H., Xu, Z.G., Yang, Z.H., 2009. Three-layer model for ver-
507 tical velocity distribution in open channel flow with submerged rigid vegeta-
508 tion. Advances in Water Resources 32, 487–492. doi:10.1016/j.advwatres.
509 2008.11.014.

510 Huai, W.X., Zhang, J., Katul, G., Cheng, Y.G., Tang, X., Wang, W.J., 2019.
511 The structure of turbulent flow through submerged flexible vegetation. Jour-
512 nal of Hydrodynamics 31, 774–781. doi:10.1007/s42241-019-0023-3.

513 Ishikawa, Y., Mizuhara, K., Ashida, S., 2000. Effect of density of trees on drag
514 exerted on trees in river channels. Journal of Forest Research 5, 271–279.
515 doi:10.1007/BF02767121.

516 James, C., Birkhead, A., Jordanova, A., O'sullivan, J., 2004. Flow resistance
517 of emergent vegetation. Journal of Hydraulic Research 42, 390–398. doi:10.
518 1080/00221686.2004.9728404.

519 Katul, G.G., Mahrt, L., Poggi, D., Sanz, C., 2004. One-and two-equation models
520 for canopy turbulence. Boundary-Layer Meteorology 113, 81–109.

Katul, G.G., Poggi, D., Ridolfi, L., 2011. A flow resistance model for assessing the impact of vegetation on flood routing mechanics. Water Resources Research 47. doi:10.1029/2010WR010278.

Katul, G.G., Wiberg, P., Albertson, J., Hornberger, G., 2002. A mixing layer theory for flow resistance in shallow streams. Water Resources Research 38. doi:10.1029/2001WR000817.

Klopstra, D., Barneveld, H., Van Noortwijk, J., Van Velzen, E., 1996. Analytical model for hydraulic roughness of submerged vegetation, in: 27th IAHR Congress, HKV Consultants. pp. 775–780.

Kothyari, U.C., Hayashi, K., Hashimoto, H., 2009. Drag coefficient of unsubmerged rigid vegetation stems in open channel flows. Journal of Hydraulic Research 47, 691–699. doi:10.3826/jhr.2009.3283.

Kouwen, N., Li, R., 1980. Biomechanics of vegetative channel linings. J. Hydraul. Div 106, 1085–1103.

Kouwen, N., Unny, T., Hill, H.M., 1969. Flow retardance in vegetated channels. Journal of the Irrigation and Drainage Division 95, 329–344.

Lee, J., Roig, L., Jenter, H., Visser, H., 2004. Drag coefficients for modeling flow through emergent vegetation in the florida everglades. Ecological Engineering 22, 237–248. doi:10.1016/j.ecoleng.2004.05.001.

Li, Z., Liu, X., Niu, T., Zhou, Q., Ma, T., Gao, Y., 2015. Ecological restoration and its effects on a regional climate: The source region of the yellow river, china. Environmental Science Technology 49, 5897.

Liu, D., Diplas, P., Fairbanks, J.D., Hodges, C.C., 2008. An experimental study of flow through rigid vegetation. Journal of Geophysical Research: Earth Surface 113. URL: http://dx.doi.org/10.1029/2008JF001042, doi:10.1029/2008JF001042.

Liu, D., Diplas, P., Hodges, C.C., Fairbanks, J.D., 2010. Hydrodynamics of flow through double layer rigid vegetation. Geomorphology 116, 286–296.

Liu, Z.W., Chen, Y.C., Zhu, D.J., Hui, E.Q., Jiang, C.B., 2011. Vertical profile of horizontal velocity of flow through shrubs (in chinese). Journal of Hydroelectric Engineering 30, 237–241.

Liu, Z.W., Chen, Y.C., Zhu, D.J., Hui, E.Q., Jiang, C.B., 2012. Analytical model for vertical velocity profiles in flows with submerged shrub-like vegetation. Environmental Fluid Mechanics 12, 341–346. doi:10.1007/s10652-012-9243-6.

Lu, J., Dai, H.C., 2016. Large eddy simulation of flow and mass exchange in an embayment with or without vegetation. Applied Mathematical Modelling 40, 7751–7767.

Luhar, M., Rominger, J., Nepf, H.M., 2008. Interaction between flow, transport and vegetation spatial structure. Environmental Fluid Mechanics 8, 423–439.

Mi, Y., He, C., Bian, H., Cai, Y., Sheng, L., Liang, M., 2015. Ecological engineering restoration of a non-point source polluted river in northern china. Ecological Engineering 76, 142–150.

Nepf, H.M., 1999. Drag, turbulence, and diffusion in flow through emergent vegetation. Water Resources Research 35, 479–489. doi:10.1029/1998WR900069.

Nepf, H.M., 2012. Flow and transport in regions with aquatic vegetation. Annual Review of Fluid Mechanics 44, 123–142. doi:10.1146/annurev-fluid-120710-101048.

Nepf, H.M., Ghisalberti, M., 2008. Flow and transport in channels with submerged vegetation. Acta Geophysica 56, 753–777. doi:10.2478/s11600-008-0017-y.

Nepf, H.M., Vivoni, E.R., 2000. Flow structure in depth-limited, vegetated flow. Journal of Geophysical Research: Oceans 105, 28547–28557. doi:10.1029/2000JC900145.

Okamoto, T.A., Nezu, I., 2009. Turbulence structure and monami phenomena in flexible vegetated open-channel flows. Journal of Hydraulic Research 47, 798–810.

Peters, T., 2012. Turbulence, coherent structures, dynamical systems and symmetry, 2nd edn., by p. holmes. Contemporary Physics 53, 1–1.

Poggi, D., Katul, G., Albertson, J., 2004a. Momentum transfer and turbulent kinetic energy budgets within a dense model canopy. Boundary-Layer Meteorology 111, 589–614. doi:10.1023/B:BOUN.0000016502.52590.af.

Poggi, D., Krug, C., Katul, G.G., 2009. Hydraulic resistance of submerged rigid vegetation derived from first-order closure models. Water Resources Research 45. doi:10.1029/2008WR007373.

Poggi, D., Porporato, A., Ridolfi, L., Albertson, J., Katul, G., 2004b. The effect of vegetation density on canopy sub-layer turbulence. Boundary-Layer Meteorology 111, 565–587. doi:10.1023/B:BOUN.0000016576.05621.73.

Shimizu, Y., Tsujimoto, T., Nakagawa, H., Kitamura, T., 1991. Experimental study on flow over rigid vegetation simulated by cylinders with equi-spacing, in: Proceedings of the Japan Society of Civil Engineers, pp. 31–40.

Stoesser, T., Kim, S., Diplas, P., 2010. Turbulent flow through idealized emergent vegetation. Journal of Hydraulic Engineering 136, 1003–1017. doi:10.1061/(ASCE)HY.1943-7900.0000153.

Stoesser, T., Salvador, G.P., Rodi, W., Diplas, P., Shavit, U., 2009. Large eddy simulation of turbulent flow through submerged vegetation. Transport in Porous Media 78, 347–365.

Stromberg, J.C., 2001. Restoration of riparian vegetation in the south-western united states: importance of flow regimes and fluvial dynamism. J Arid Ent 49, 17–34.

Tanino, Y., Nepf, H.M., 2008. Laboratory investigation of mean drag in a random array of rigid, emergent cylinders. Journal of Hydraulic Engineering 134, 34–41. doi:10.1061/(ASCE)0733-9429(2008)134:1(34).

Thom, A., 1971. Momentum absorption by vegetation. Quarterly Journal of the Royal Meteorological Society 97, 414–428.

Thompson, S., Katul, G., Konings, A., Ridolfi, L., 2011. Unsteady overland flow on flat surfaces induced by spatial permeability contrasts. Advances in Water Resources 34, 1049–1058. doi:10.1016/j.advwatres.2011.05.012.

Van Velzen, E., Jesse, P., Cornelissen, P., Coops, H., 2003. Hydraulic resistance of vegetation in floodplains, part 2: Background document version 1-2003. Ministry of Transport, Public Works and Water Management, Institute for Inland Water Management and Waste Water Treatment, report .

Wang, W., 2012. An analytical model for mean wind profiles in sparse canopies. Boundary-Layer Meteorology 142, 383–399.

Wang, W.J., Huai, W.X., Thompson, S., Katul, G.G., 2015a. Steady nonuniform shallow flow within emergent vegetation. Water Resources Research 51, 10047–10064. doi:10.1002/2015WR017658.

Wang, W.J., Huai, W.X., Thompson, S., Peng, W.Q., Katul, G.G., 2018a. Drag coefficient estimation using flume experiments in shallow non-uniform water flow within emergent vegetation during rainfall. Ecological Indicators 92, 367–378. doi:10.1016/j.ecolind.2017.06.041.

Wang, W.J., Huai, W.X., Zeng, Y.H., Zhou, J.F., 2015b. Analytical solution of velocity distribution for flow through submerged large deflection flexible vegetation. Applied Mathematics and Mechanics 36, 107–120. doi:10.1007/s10483-015-1897-9.

Wang, W.J., Peng, W.Q., Huai, W.X., Katul, G., Liu, X.B., Dong, F., Qu, X.D., Zhang, H.P., 2018b. Derivation of canopy resistance in turbulent flow from first-order closure models. Water 10, 1782. doi:10.3390/w10121782.

Wang, W.J., Peng, W.Q., Huai, W.X., Katul, G., Liu, X.B., Qu, X.D., Dong, F., 2019. Friction factor for turbulent open channel flow covered by vegetation. Scientific Reports , 5178.

Wang, W.J., Peng, W.Q., Huai, W.X., Qu, X.D., Dong, F., Feng, J., 2018c. Roughness height of submerged vegetation in flow based on spatial structure. Journal of Hydrodynamics 30, 754–757. doi:10.1007/s42241-018-0060-3.

Yang, W., Choi, S.U., 2010. A two-layer approach for depth-limited open-channel flows with submerged vegetation. Journal of Hydraulic Research 48, 466–475. doi:10.1080/00221686.2010.491649.

Yu, S., Wang, M., 2014. Comprehensive evaluation of scenario schemes for multi-objective decision-making in river ecological restoration by artificially recharging river. Water Resources Management 28, 5555–5571.

Zhang, M., Hao, Z., Zhang, Y., Wu, W., 2013. Numerical simulation of solitary and random wave propagation through vegetation based on vof method. Acta Oceanologica Sinica 32, 38–46.

View publication stats